The Astrophysical Journal, 628:555–566, 2005 July 20

INVESTIGATION OF THE ULTRAVIOLET, VISIBLE, AND NEAR-INFRARED ABSORPTION SPECTRA OF HYDROGENATED POLYCYCLIC AROMATIC HYDROCARBONS AND THEIR CATIONS

T. M. Halasinski,[1] F. Salama,[2] and L. J. Allamandola
NASA Ames Research Center, Mail Stop 245-6, Moffett Field, CA 94035-1000
Received 2004 November 24; accepted 2005 March 26

ABSTRACT

The formation and the presence of PAHs containing excess H atoms, or hydrogenated PAHs (H_n-PAHs) in interstellar clouds has recently been discussed. It has been suggested that H_n-PAHs contribute to the IR emission bands and that they might be among the molecular precursors of the carbon particles that cause the interstellar UV extinction curve. The spectroscopy of H_n-PAHs is investigated, and the implications for interstellar spectra are discussed. The UV, visible, and near-IR absorption spectra of a series of H_n-PAHs and their photoproducts formed by vacuum UV irradiation were measured for the first time in inert-gas (neon) matrices at 5 K. It is shown that the spectra of both the neutral H_n-PAH and cationic H_n-PAH$^+$ species exhibit vibronic band systems with similar spectral positions and relative spectral intensities to their nonhydrogenated PAH chromophore counterparts. The results are discussed in the context of the nature of the origin of the diffuse interstellar bands.

Subject headings: astrochemistry — ISM: lines and bands — ISM: molecules — methods: laboratory — molecular data — ultraviolet: ISM

1. INTRODUCTION

One of the most ubiquitous spectral signatures of interstellar molecules is a set of IR emission bands, the unidentified infrared bands (UIRs), which are observed at 3.3, 6.2, 7.7, 8.6, and 11.2 μm (Gillett et al. 1973). While it has proved difficult to unambiguously identify the individual molecular species responsible for the UIRs, there is now strong evidence that these emission features arise from carbonaceous aromatic materials and, in particular, from a distribution of neutral and ionized polycyclic aromatic hydrocarbons (PAHs; Allamandola et al. 1999). PAHs are considered good candidates because they are stable against UV photodissociation, a requirement to maintain the concentration necessary in the interstellar medium (ISM), where materials are exposed to harsh far-UV radiation fields. This is particularly true for the diffuse medium, where neutral and ionic PAHs are thought to contribute to the diffuse interstellar bands (DIBs). DIBs are absorption bands from the near-UV to the near-IR seen in the spectra of stars that are obscured by diffuse interstellar molecular clouds (Snow 2001). Although a specific molecular carrier—or a class of molecular carriers—is yet to be unambiguously identified, laboratory studies have shown that several of the observed vibronic transitions of PAH ions are found in the same spectral region where the known DIBs are located and can therefore be considered as good candidates for the origin of some of these astronomical features (Salama et al. 1999; Ruiterkamp et al. 2002).

While the IR emission from interstellar sources strongly suggests the presence of PAHs, it is difficult to extend this hypothesis to include information on which individual PAHs may be found there. The information that is obtained from IR bands only includes the family of structures; little information is provided about *individual* molecular structures. The absorption arising from electronic transitions, on the other hand, can offer much more specific information regarding the nature of the molecular carrier than the IR emission bands. Thus, identification of the DIBs in the near-UV to the near-IR range offers the potential for a much more complete picture of which specific molecules can be found in diffuse molecular clouds. A more complete understanding of the chemistry that occurs within these regions can be obtained only after specific molecular information is known.

Although individual PAHs have yet to be unambiguously identified within the interstellar medium, current experimental as well as theoretical research is focused on the spectral signatures of the many possible different structural variants of PAHs that may exist in these regions. This includes examining spectral signatures as a function of molecular size (Ruiterkamp et al. 2002; Bauschlicher 2002; Weisman et al. 2003), charge (cations and anions; Halasinski et al. 2000), multiply charged ions (Bakes et al. 2001), the addition of oxygen-containing side groups (Bauschlicher 1998a), the addition of nitrogen-containing side groups as well as nitrogen substitution within the PAH ring (Bauschlicher 1998b; Mattioda et al. 2003), PAHs containing non–six-membered rings (nonbenzenoid structures; Bauschlicher et al. 1999; Hudgins et al. 2000; Pauzat & Ellinger 2002), open/closed-shell molecular systems (Weisman et al. 2001; Hudgins et al. 2001), and degree of hydrogenation—due to addition of methyl and/or aliphatic substituents to the PAH (Jochims et al. 1999; Pauzat & Ellinger 2001; Petrie et al. 2003) as well as the addition of protons to the PAH (Snow et al. 1998; Bauschlicher 1998c; Le Page et al. 1999; Herbst & Le Page 1999; Bauschlicher & Bakes 2001).

In this report, we discuss PAHs containing excess H atoms (H_n-PAHs; see Figs. 1 and 2). More specifically, we focus on a subset of H_n-PAHs (and their cations) in which an even number of hydrogen atoms have been added to an even number of carbon atoms (Fig. 1) and an odd number of hydrogen atoms have been added to an odd number of carbon atoms (Fig. 2). Thus, the molecules considered here are closed shell in their neutral form and open shell in their singly ionized cationic form. This is the first time that the electronic spectra of these H_n-PAHs are reported in the literature. We do not focus on species containing an even number of carbon atoms and an odd number of hydrogen atoms (see Fig. 1) or on species containing an odd number of carbon atoms and an even number of hydrogen atoms (see Fig. 2), as these species are difficult to prepare in situ using matrix isolation.

[1] Current address: Department of Chemistry, Saint Joseph's University, Philadelphia, PA 19131.
[2] Corresponding author: farid.salama@nasa.gov.

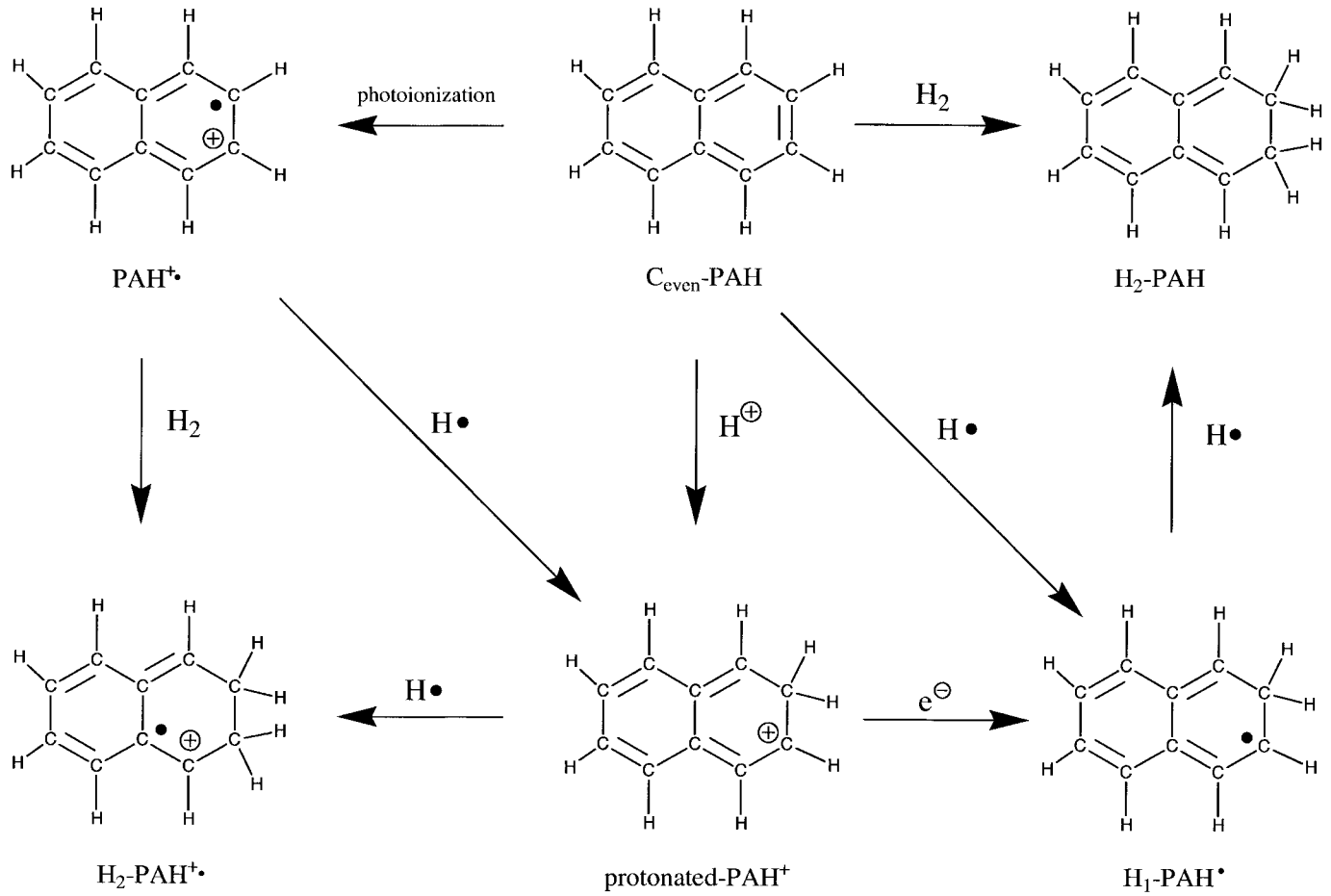

FIG. 1.—Representative structure of a fully aromatic PAH with an even number of carbon atoms and its partially aromatic H_n-PAH and protonated PAH counterparts.

Included in this study are naphthalene ($C_{10}H_8$), phenanthrene ($C_{14}H_{10}$), and pyrene ($C_{16}H_{10}$), which are fully aromatic PAHs. Accordingly, the acenaphthene ($C_{12}H_{10}$) compound can be considered to be an H_n-PAH in which two hydrogen atoms have been added to acenaphthylene ($C_{12}H_8$). Thus, this molecule can be designated as an H_2-PAH. Hexahydropyrene ($C_{16}H_{16}$) can be considered as an H_6-PAH. The molecule 4,5-dihydropyrene ($C_{16}H_{12}$) can be designated as an H_2-PAH, and 7,8,9,10-tetrahydrobenzo[*a*]pyrene ($C_{20}H_{16}$) can be designated as an H_4-PAH. The species 4*H*-cyclopenta[*def*]phenanthrene ($C_{15}H_{10}$), 5,6-dihydro-4*H*-benz[*de*]anthracene ($C_{17}H_{14}$), and 7,8-dihydro-9*H*-cyclopenta[*a*]pyrene ($C_{19}H_{14}$) do not have fully aromatic PAH counterparts; however, as they do contain both aromatic and aliphatic features within their molecular structure, we also refer to them as H_n-PAHs in this report.

Theoretical modeling (Duley & Williams 1981; Schutte et al. 1993) combined with astronomical observations of the interstellar IR emission (Jourdain de Muizon et al. 1986) has led to the suggestion that H_n-PAHs might be the potential carriers of the weaker UIR bands in the 3–4 μm region. Subsequent studies combining laboratory measurements of the IR absorption spectra of H_n-PAHs isolated in argon matrices (Bernstein et al. 1996) with astronomical observations of the Orion Bar (Sloan et al. 1997) have shown that H_n-PAHs could well account for the weak UIR bands observed in the 3.35–3.60 μm range. Furthermore, mixtures of H_n-PAHs exposed to hydrogen plasmas in the laboratory (Beegle et al. 1997a, 1997b, 2001; Arnoult et al. 2000) lead to the formation of larger hydrogenated structures with spectral characteristics close to interstellar UV and IR signatures. Recent detailed studies of the IR emission spectra of gas-phase H_n-PAHs (Wagner et al. 2000) show that H_n-PAHs produce a good match to the interstellar bands in the 3.3–3.6 μm range (i.e., the "satellite" UIR bands), while making little contribution to the other UIR bands.

The focus of this paper is to investigate for the first time the spectroscopy of neutral and ionized H_n-PAHs in the UV to near-IR range and to examine the astrophysical implications. It is shown that the spectra of neutral and ionized H_n-PAHs do not greatly differ from the spectral characteristics of their chromophores in this region of the spectrum. A chromophore can be defined as a group of atoms in a molecule that serve as a unit of light absorption. In the molecules discussed here, the chromophore is the portion of the molecule where the electrons are delocalized in π orbitals, i.e., the aromatic portion of the molecule. The results are discussed in terms of their context to the nature of the carriers of the DIBs.

2. EXPERIMENTAL

The laboratory spectra were obtained using the technique of matrix isolation spectroscopy (MIS). This technique approximates the known (or expected) environmental conditions of the diffuse interstellar medium in the laboratory. In MIS experiments, neutral and ionized H_n-PAHs are fully isolated in low-polarizability neon matrices at $\sim$5 K. The induced perturbations—in terms of peak position and profile of the bands—in the spectra of the neutral/ionized H_n-PAHs are minimized in neon matrices as compared to matrices composed of argon or krypton (Salama 1996). The experimental instrumentation employed in these

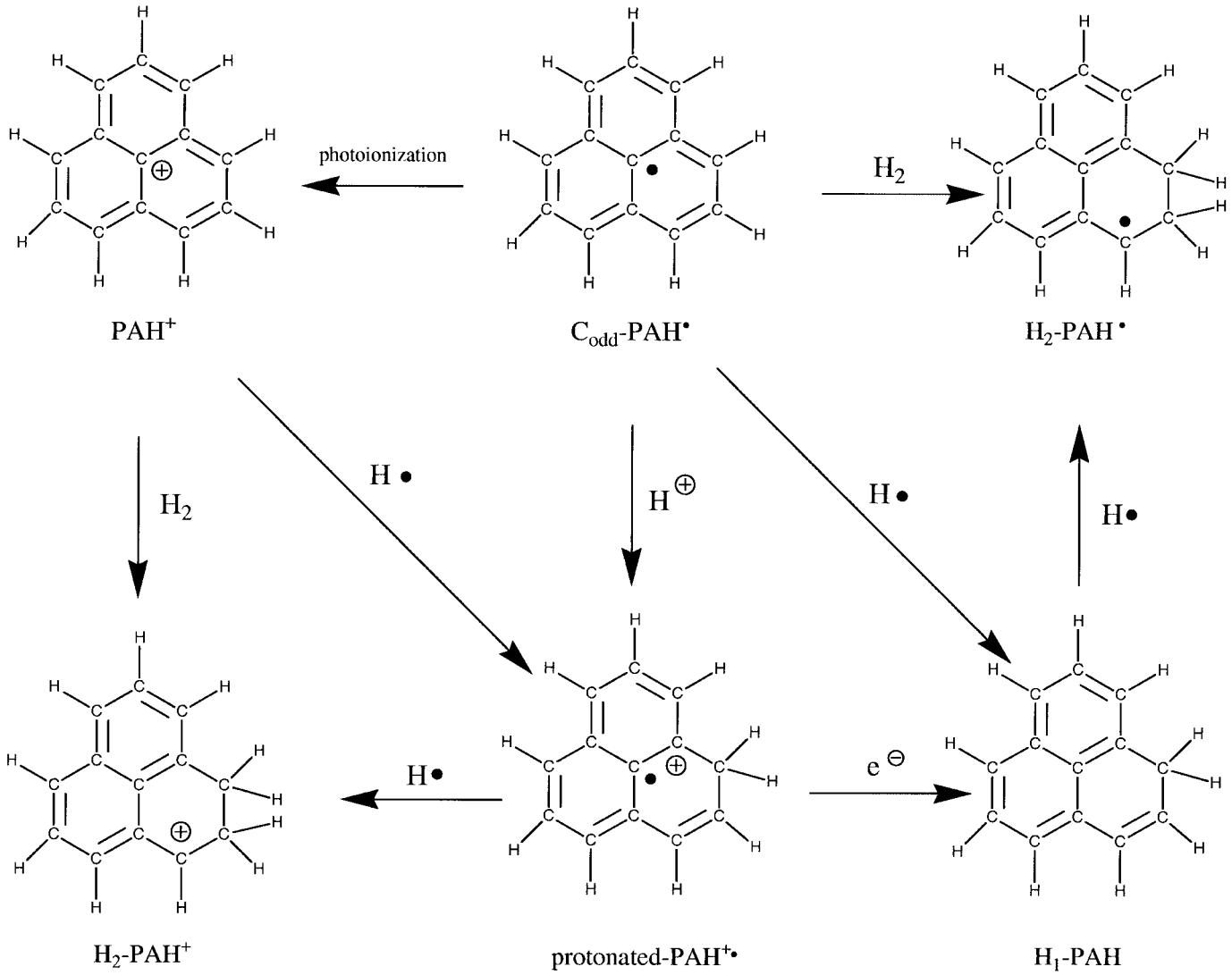

FIG. 2.—Representative structure of a fully aromatic PAH with an odd number of carbon atoms and its partially aromatic H_n-PAH and protonated PAH counterparts.

studies, a UV/visible/near-IR spectrometer equipped with its own dedicated sample vacuum chamber and matrix deposition source, has been previously described (Salama & Allamandola 1991; Salama et al. 1994). A brief review will be given here.

The UV/visible/near-IR instrument is equipped with a sapphire sample window cooled to 4.2 K by an extended liquid helium transfer cryostat. The sample window can be rotated 360° under vacuum to face, alternatively, two spectroscopic window ports, the matrix gas and H_n-PAH deposition lines, and a MgF_2 vacuum UV window port.

Single-beam spectra of the cold substrate were collected before the matrix was deposited and were used as the background for all spectra reported, unless noted otherwise. A deuterium lamp provides spectral output from 160 to 360 nm, and a quartz tungsten halogen lamp provides output from 320 to 2500 nm. Spectra of the isolated H_n-PAH molecules and ions were recorded from 180 to 1000 nm with a nominal resolution of 0.1 nm using a 0.5 m, triple grating monochromator and a CCD camera array mounted on the exit port and interfaced to a computer system.

The vaporization and codeposition of each H_n-PAH with the inert gas (neon) was performed using Pyrex tubes (12.7 mm outer diameter), which were mounted on the sample chamber through a stainless steel Ultra-Torr fittings and heated from outside the vacuum chamber with the use of heating tape. The tubes were positioned between 4 and 5 cm from the cold window and perpendicular to the surface of the cold substrate. The temperature of the tube was monitored using a chromel/alumel thermocouple mounted on the exterior of each tube with Al foil tape.

Matrix gas was admitted through a port at a position 45° from the plane of the substrate surface and the median between the Pyrex tube containing the PAH sample such that the two vapor streams combined before the surface of the window. Ne flow rates were estimated to be 12 mmol hr^{-1}. Based on these flow rates and vaporization temperatures, the matrix/PAH ratio is estimated to be in excess of 1000/1. Typical deposition times varied from 2 to 4 hr.

A microwave-powered hydrogen flow (10% H_2/He) discharge lamp (Opthos Instruments MPG 4M) mounted on the MgF_2 vacuum chamber window was used for photolysis of the matrix to form the molecular ions in situ. This lamp generates nearly monochromatic radiation in the Lyα line at 121.6 nm (10.2 eV). Typical photolysis times ranged from 2 to 20 minutes.

The H_n-PAHs were obtained from Ronald Harvey (The Ben May Institute for Cancer Research, University of Chicago), while the non–H_n-PAHs were obtained from Aldrich chemical. The chemicals from both sources were used as received.

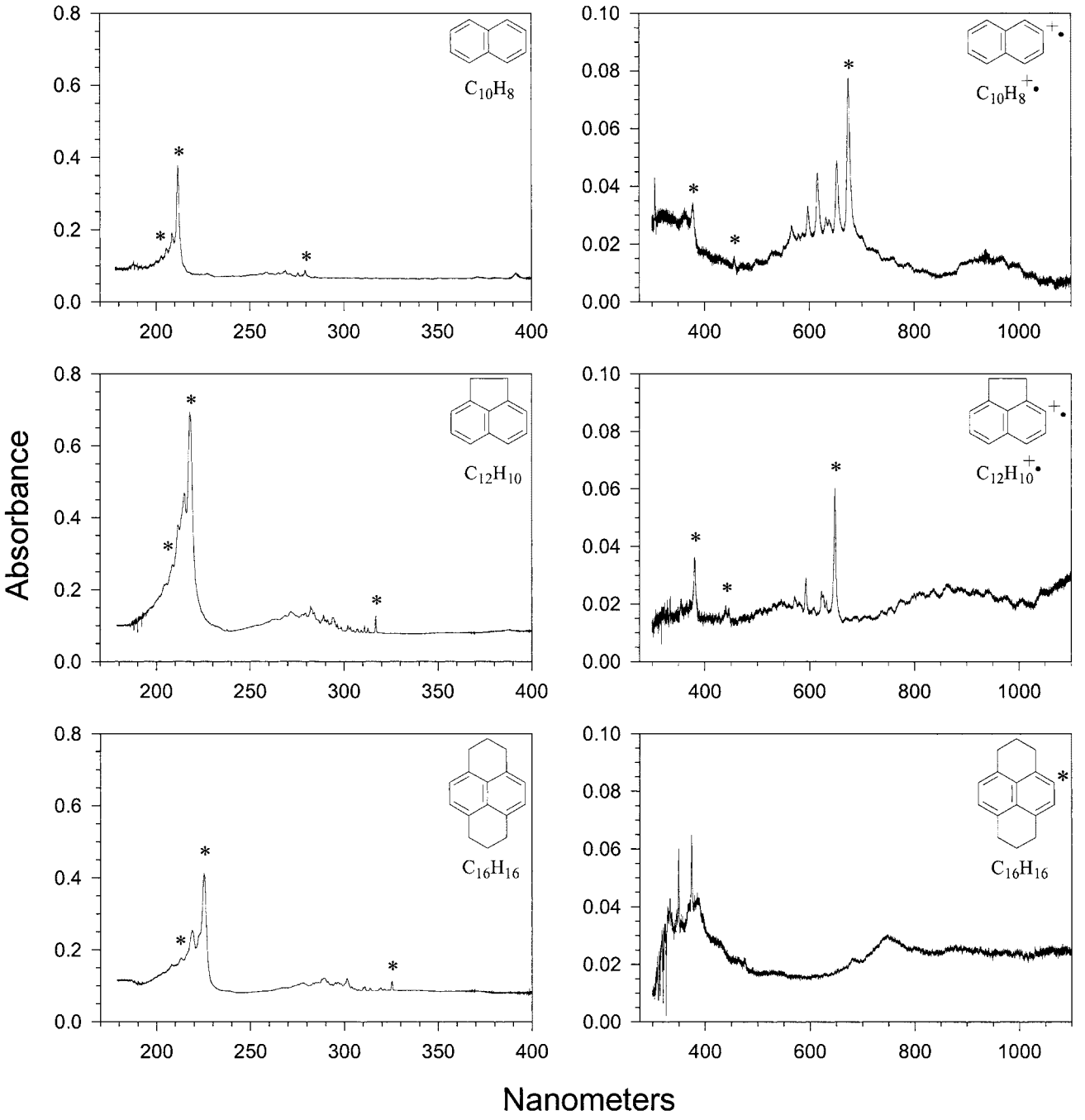

FIG. 3.—Spectra for the PAH neutral molecules, cations, and photofragments containing the naphthalene chromophore. The bands marked with an asterisk are assigned to an electronic origin within the molecule or ion.

Ne (Cryogenic Rare Gas 99.9995%) research grade rare gas was used without further purification. All depositions were repeated with CCl_4-doped matrix gas (a well-known electron acceptor) to ensure that spectral features assigned to photoproducts could be assigned to cationic species.

3. RESULTS

The laboratory spectra measured in the near-UV to near-IR range (180–1000 nm) are shown in Figures 3–5. For comparison and clarity purposes, the spectra have been arranged according to their respective aromatic chromophore (i.e., regular PAH). Thus, each figure displays the aromatic chromophore spectrum on top with the spectra of its H_n-PAH counterparts containing the specific aromatic chromophore below. Figure 3 is associated with the naphthalene chromophore ($C_{10}H_8$), Figure 4 with the phenanthrene chromophore ($C_{10}H_{14}$), and Figure 5 with the pyrene chromophore ($C_{16}H_{10}$). The positions and relative intensities of the spectral bands associated with the spectra shown in Figures 3–5 are listed in Tables 1–3. For the most part, the spectra clearly illustrate the similarity between the energy levels of the π–π^* electronic transitions of the H_n-PAHs to that of their respective PAH chromophore counterparts. It should be noted here that while the neutral PAH molecules studied here only exhibit singlet electronic transitions to excited states in the UV spectral region, the

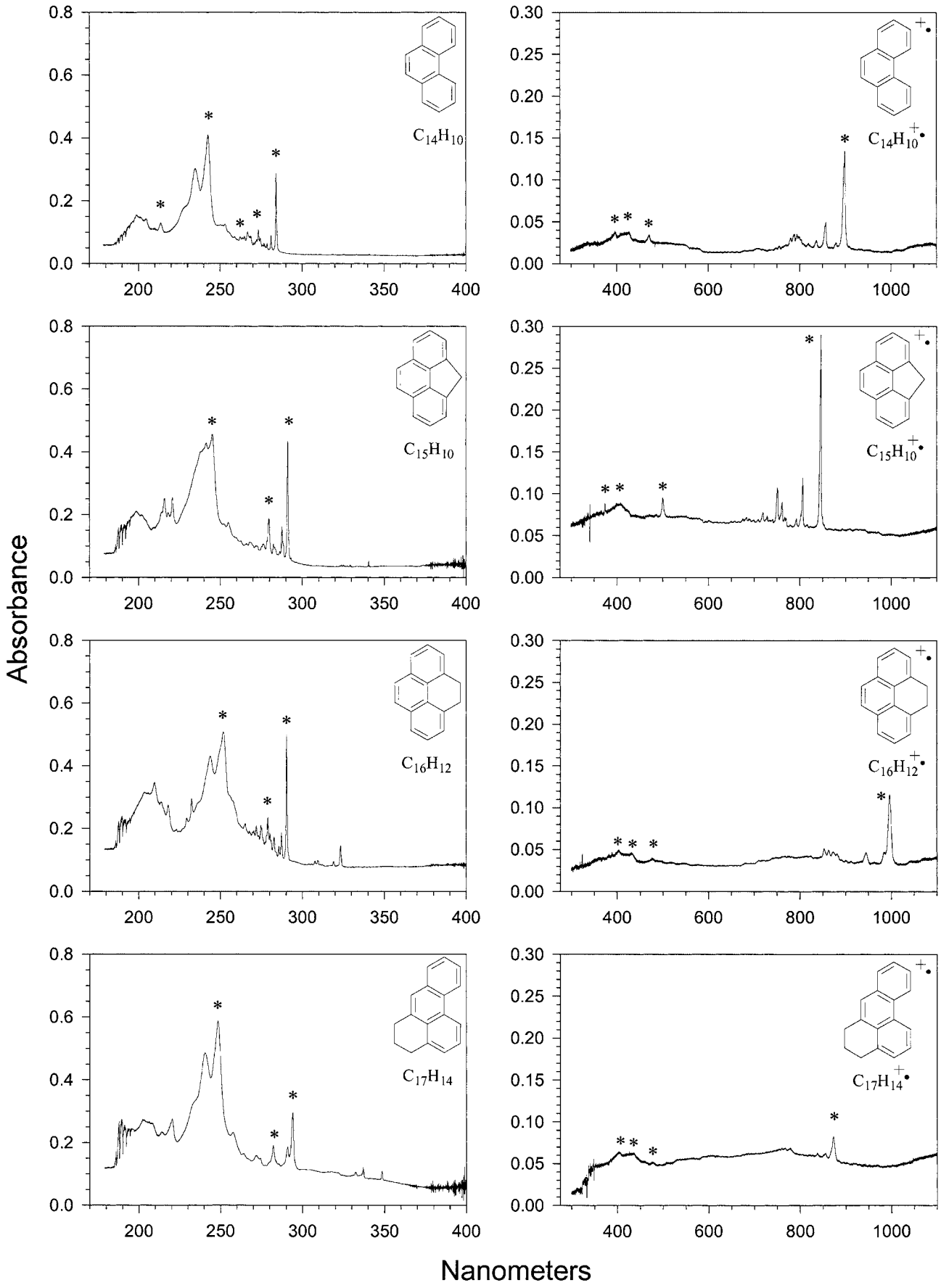

FIG. 4.—Spectra for the PAH neutral molecules and cations containing the phenanthrene chromophore. The bands marked with an asterisk are assigned to an electronic origin within the molecule or ion.

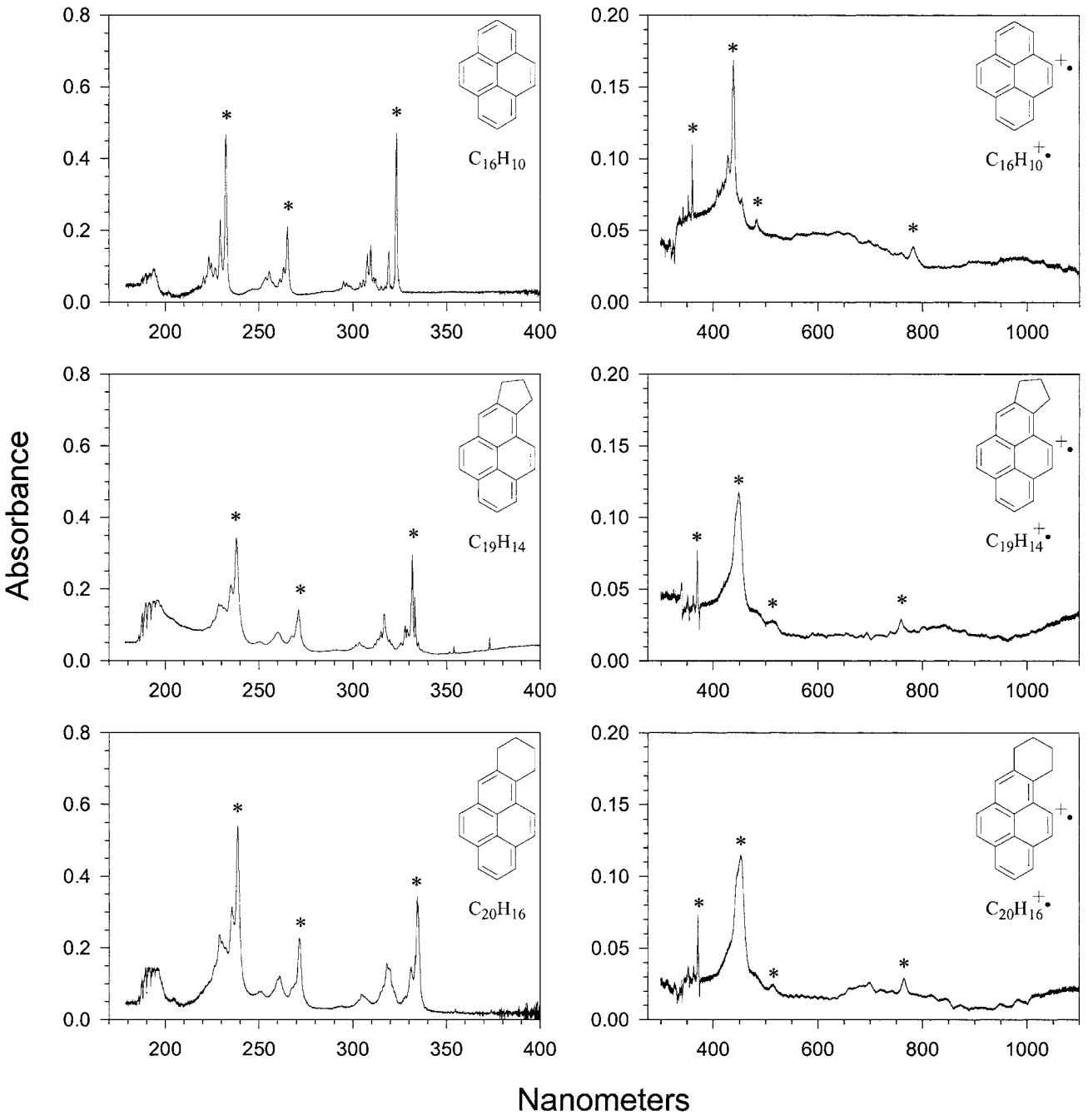

FIG. 5.—Spectra for the PAH neutral molecules and cations containing the pyrene chromophore. The bands marked with an asterisk are assigned to an electronic origin within the molecule or ion.

PAH ions are expected to exhibit spectral transitions in both the visible and the UV region (Chillier et al. 1999). In matrix isolation experiments, the ionization yield is generally low (5%–10%), and the UV absorption bands of the neutral precursor molecules strongly obscure the much weaker absorptions associated with the ions. We therefore only examine the PAH ion absorptions in the visible region for the experiments reported here.

4. DISCUSSION—SPECTROSCOPY

The observed features in the spectral regions displayed in Figures 3–5 arise from the promotion of electrons from π bonding orbitals to π antibonding orbitals. Transitions involving the promotion of electrons between σ and σ^* orbitals are expected to lie at much higher energy levels than can be measured with our current spectrometer ($\sim$vacuum UV region). Thus, the spectral characteristics of the molecules in this study are determined in a large part by the aromatic portion of the molecule. Following the convention adopted in the figures and tables, the discussion is also ordered according to the nature of the aromatic chromophore (§ 4.1, the naphthalene chromophore [$C_{10}H_8$]; § 4.2, the phenanthrene chromophore [$C_{10}H_{14}$]; and § 4.3, the pyrene chromophore [$C_{16}H_{10}$]). Whenever possible, we include wavelength values from measurements taken in the gas phase when they occur in the same spectral region as the DIBs.

TABLE 1

SPECTRAL DATA FOR THE PAH NEUTRAL MOLECULES, CATIONS, AND PHOTOPRODUCTS CONTAINING THE NAPHTHALENE CHROMOPHORE

Species	Assignment	Position (nm)	Shift (cm^{-1})	Maximum Absorbance
Naphthalene				
($C_{10}H_8$)		201.9	437	0.074
	$4 \leftarrow 0$	203.7	0	0.121
		205.7	1355	0.199
		208.9	611	0.357
	$3 \leftarrow 0$	211.6	0	1.000
		258.3	2898	0.017
		265.5	1848	0.017
		268.5	1427	0.034
		275.4	494	0.037
	$2 \leftarrow 0$	279.2	0	0.061
Acenaphthene				
($C_{12}H_{10}$)		204.5	984	0.199
	$4 \leftarrow 0$	208.7	0	0.293
		211.5	1430	0.477
		214.9	682	0.624
	$3 \leftarrow 0$	218.1	0	1.000
		271.6	5263	0.020
		282.2	3880	0.055
		289.1	3034	0.041
		294.2	2434	0.038
		302.0	1557	0.023
		310.9	609	0.033
	$2 \leftarrow 0$	316.9	0	0.076
Hexahydropyrene				
($C_{16}H_{16}$)		208.0	1173	0.186
	$4 \leftarrow 0$	213.2	0	0.255
		219.1	1275	0.500
		222.7	537	0.463
	$3 \leftarrow 0$	225.4	0	1.000
		277.4	5318	0.025
		289.2	3847	0.065
		296.8	2962	0.031
		301.4	2448	0.075
		311.0	1423	0.037
		319.4	578	0.022
	$2 \leftarrow 0$	325.4	0	0.081
Naphthalene cation				
($C_{10}H_8^+$)	$^2B_{3g} \leftarrow 0$	305.0	414	0.308
		363.0	1016	0.115
	$4 \leftarrow 0$	376.9	0	0.231
	$3 \leftarrow 0$	456	0	0.058
		565.8	2839	0.096
		578.4	2454	0.019
		584.8	2265	0.019
		596.5	1929	0.192
		615.1	1423	0.404
		631.4	1003	0.096
		637.6	849	0.077
		652.0	502	0.462
	$2 \leftarrow 0$	674.1	0	1.000
Acenaphthene cation				
($C_{12}H_{10}^+$)		354.5	1928	0.114
	$4 \leftarrow 0$	380.5	0	0.432
		440.0	305	0.091
	$3 \leftarrow 0$	446.0	0	0.091
		571.4	2071	0.091
		582.2	1746	0.045
		592.7	1442	0.273
		608.1	1015	0.045
		622.9	624	0.159
		626.0	544	0.136
		631.7	400	0.091
	$2 \leftarrow 0$	648.1	0	1.000
Hexahydropyrene				
photoproducts ($C_{16}H_{16}^*$)		349.5	...	1.000
		374.1	...	0.889
		747.7	...	0.370

NOTE.—Only the most intense features observed are included here.

4.1. *Neutral and Ionized Naphthalene* ($C_{10}H_8$), *Acenaphthene* ($C_{12}H_{10}$), *and Neutral and Photoproducts of Hexahydropyrene* ($C_{16}H_{16}$)

The well-studied spectra of $C_{10}H_8$ and $C_{10}H_8^+\cdot$ isolated in Ne matrices (Salama & Allamandola 1991 and references therein) are illustrated in the top two panels of Figure 3, and the observed spectral positions and corresponding maximum absorbances are listed in Table 1. The dominant feature for $C_{10}H_8$ is observed at 211.6 nm and has been previously assigned to the origin of the $S_3 \leftarrow S_0$ transition. The electronic origin of the $S_4 \leftarrow S_0$ transition is observed at 203.7 nm. The much weaker spectral origin for the $S_2 \leftarrow S_0$ transition is observed at 279.2 nm, and the origin for the $S_1 \leftarrow S_0$ transition previously observed at 311.5 nm is too weak to observe in the experiments reported here. In each observed electronic transition, one or more features due to vibronic transitions are also observed.

The dominant features in the $C_{10}H_8^+\cdot$ spectrum (500–700 nm) are due to the electronic origin and vibronic transitions of $D_2 \leftarrow D_0$ (Salama & Allamandola 1991). The electronic origin and the lowest energy vibronic transition, 674.1 and 652.0 nm, respectively, have been recently measured in the gas phase at 670.6 and 648.9 nm, respectively (Romanini et al. 1999; Pino et al. 1999; Biennier et al. 2003). The feature lying near 456 nm has been assigned to the electronic origin of the $D_3 \leftarrow D_0$ transition and was also recently measured in the gas phase at 454.9 nm (Pino et al. 1999). The electronic origin of the $D_4 \leftarrow D_0$ transition is observed at 376.9 nm. The feature lying highest in energy (305.0 nm) in the given spectral region has also been assigned to a vibronic promotion of the $B_{3g} \leftarrow X\,^2A_u(D_0)$ electronic transition. The electronic origin of this particular transition is presumably too weak to observe in these experiments.

The similarity of the $C_{10}H_8$ spectrum to the $C_{12}H_{10}$ spectrum and that of the $C_{10}H_8^+\cdot$ spectrum to the $C_{12}H_{10}^+\cdot$ spectrum allows us to tentatively assign some of the features in the $C_{12}H_{10}/C_{12}H_{10}^+\cdot$ spectra. We assign the most intense feature in the $C_{12}H_{10}$ spectrum at 218.1 nm to the electronic origin of the $S_3 \leftarrow S_0$ transition and the features at 214.9 and 211.5 nm to vibronic promotions within

TABLE 3

SPECTRAL DATA FOR THE PAH NEUTRAL MOLECULES AND CATIONS CONTAINING THE PYRENE CHROMOPHORE

Species	Assignment	Position (nm)	Shift (cm^{-1})	Maximum Absorbance
Pyrene ($C_{16}H_{10}$)		223.2	1755	0.250
		229.3	563	0.473
	4 ← 0	232.3	0	1.000
		255.5	1432	0.147
		263.1	301	0.174
	3 ← 0	265.2	0	0.426
		307.8	1558	0.234
		309.4	1390	0.292
		319.1	407	0.257
	2 ← 0	323.3	0	0.971
7,8-Dihydro-9*H*-cyclopenta[*a*]pyrene ($C_{19}H_{14}$)		228.6	1728	0.307
		235.1	518	0.523
	4 ← 0	238.0	0	1.000
		260.1	1560	0.143
		267.2	538	0.122
	3 ← 0	271.1	0	0.383
		315.0	1607	0.209
		316.8	1427	0.369
		328.0	349	0.265
	2 ← 0	331.8	0	0.951
7,8,9,10-Tetrahydrobenzo[*a*]pyrene ($C_{20}H_{16}$)		229.0	1757	0.398
		235.6	534	0.555
	4 ← 0	238.6	0	1.000
		261.0	1495	0.175
		269.2	328	0.129
	3 ← 0	271.6	0	0.390
		318.1	1524	0.256
		319.6	1376	0.225
		330.9	308	0.239
	2 ← 0	334.3	0	0.622
Pyrene cation ($C_{16}H_{10}^{+}$)		342.5	1412	0.090
		352.6	576	0.153
	6 ← 0	359.9	0	0.459
		408.1	1709	0.144
		417.8	1140	0.189
		428.4	548	0.378
	5 ← 0	438.7	0	1.000
		454.7	1302	0.153
	4 ← 0	483.3	0	0.063
	2 ← 0	781.6	0	0.099
7,8-Dihydro-9*H*-cyclopenta[*a*]pyrene cation ($C_{19}H_{14}^{+}$)		351.0	1434	0.114
		361.8	584	0.101
	6 ← 0	369.6	0	0.494
	5 ← 0	447.5	0	1.000
	4 ← 0	512.3	0	0.063
	2 ← 0	758.7	0	0.127
7,8,9,10-Tetrahydrobenzo[*a*]pyrene cation ($C_{20}H_{16}^{+}$)		352.0	1418	0.102
		362.5	595	0.114
	6 ← 0	370.5	0	0.511
	5 ← 0	452.7	0	1.000
	4 ← 0	513.6	0	0.057
	2 ← 0	764.6	0	0.125

NOTE.—Only the most intense features observed are included here.

the S_3 excited state. The feature at 316.9 nm can be readily assigned to the electronic origin of the $S_2 \leftarrow S_0$ transition. Several features are also observed that can be assigned to vibronic promotions within the $S_2 \leftarrow S_0$ transition. The feature at 208.7 nm can be tentatively assigned to the electronic origin of the $S_4 \leftarrow S_0$ transition along with a vibronic promotion at 204.5 nm. Presumably, the electronic origin of the $S_1 \leftarrow S_0$ transition is too weak to observe in these experiments.

In a similar manner, we tentatively assign the dominant spectral features lying at 648.1, 626.0, 622.9, and 592.7 nm in the $C_{12}H_{10}^{+}\cdot$ spectrum to a vibronic progression within the $D_2 \leftarrow D_0$ transition. The origin of this vibronic progression has been recently measured in the gas phase at 646.3 nm (Biennier et al. 2003). The spectral feature at 446.0 nm can be assigned to the electronic origin of the $D_3 \leftarrow D_0$ transition, and the feature at 380.5 nm to the origin of the $D_4 \leftarrow D_0$ transition. Similar transitions for the $C_{12}H_{10}^{+}\cdot$ cation isolated in argon matrices have been recently assigned (Banisaukas et al. 2003).

Neutral hexahydropyrene, $C_{16}H_{16}$, also follows the same trend discussed above. Based on the previously assigned spectrum of naphthalene, we assign the bands observed at 325.4, 225.4, and 213.2 nm in the $C_{16}H_{16}$ spectrum to the electronic origins of the $S_2 \leftarrow S_0$, $S_3 \leftarrow S_0$, and $S_4 \leftarrow S_0$ transitions for that molecule. The spectral origin of the $S_1 \leftarrow S_0$ transition is too weak to observe in the experiments reported here.

In contrast to the cases of $C_{10}H_8$ and $C_{12}H_{10}$, where vacuum UV irradiation leads to photoionization (formation of $C_{10}H_8^{+}\cdot$ and $C_{12}H_{10}^{+}\cdot$), the spectra observed after vacuum UV irradiation of $C_{16}H_{16}$ seem to indicate the photofragmentation of the neutral precursor. The spectrum of irradiated $C_{16}H_{16}$ shown in Figure 3 clearly departs from the structural pattern observed for all other series containing the same PAH chromophore. In addition, the bands observed at 374.1 and 349.5 nm grow at different rates with the energy of photolysis, indicating the possibility that more than one photoproduct of $C_{16}H_{16}$ was produced upon vacuum UV irradiation (i.e., fragmentation).

4.2. *Neutral and Ionized Phenanthrene* ($C_{14}H_{10}$), *4H-cyclopenta[def]phenanthrene* ($C_{15}H_{10}$), *4,5-dihydropyrene* ($C_{16}H_{12}$), *and 5,6-dihydrobenzo[de]anthracene* ($C_{17}H_{14}$)

The well-studied spectra of $C_{14}H_{10}$ and $C_{14}H_{10}^{+}\cdot$ isolated in Ne matrices (Salama et al. 1994 and references therein) are illustrated in the top two panels of Figure 4, and the observed spectral positions and corresponding maximum absorbances are listed in Table 2. Phenanthrene ($C_{14}H_{10}$) exhibits a relatively complex series of features within the displayed spectral region, as compared to naphthalene ($C_{10}H_8$); no less than five excited states are observed in this region (Salama et al. 1994). The first excited state at 341.1 nm is too weak to observe in the experiments reported here. The sharp spectral feature at 284.3 nm has been assigned to the electronic origin of the $S_2 \leftarrow S_0$ transition. The most intense transition at 243.0 nm has been assigned to the electronic origin of the $S_5 \leftarrow S_0$ transition. Features weaker in intensity at 273.4 and 262.4 nm have been assigned to the spectral origins of the $S_3 \leftarrow S_0$ and $S_4 \leftarrow S_0$ transitions, respectively. The shoulder at 229.0 nm has been attributed to the $S_6 \leftarrow S_0$ transition, and the feature at 214.5 nm has been assigned to the spectral origin of the $S_7 \leftarrow S_0$ transition.

All the observed spectral features with wavelengths longer than 650 nm in the $C_{14}H_{10}^{+}\cdot$ spectrum have been assigned to vibronic transitions within the $D_2 \leftarrow D_0$ transition, where the electronic origin lies at 898.3 nm. This electronic origin and the second-lowest energy vibronic transition at 856.6 nm have been recently measured in the gas phase at 891.9 and 850.8 nm, respectively (Bréchignac & Pino 1999; Bréchignac et al. 2001). The features lying at 470.7, 425.8, and 396.0 nm have been assigned to the origins of the $D_4 \leftarrow D_0$, $D_5 \leftarrow D_0$, and $D_6 \leftarrow D_0$ transitions, respectively. The origin of the $D_3 \leftarrow D_0$ transition at 634.4 nm is too weak to observe in these experiments.

As with the case of naphthalene and acenaphthene, the similarities of the spectra of phenanthrene and the compounds containing the phenanthrene chromophore allow us to assign several transitions within these species. In the neutral species containing the phenanthrene chromophore, the second, third, and fifth electronic origins are the most readily assigned. Thus, we assign the features at 291.1, 276.6, and 245.2 nm in the $C_{15}H_{10}$ spectrum to the electronic origins of the $S_2 \leftarrow S_0$, $S_3 \leftarrow S_0$, and $S_5 \leftarrow S_0$ transitions, respectively. Similarly, we assign the features at 290.4, 278.9, and 251.8 nm in the $C_{16}H_{12}$ spectrum to the electronic origins of the $S_2 \leftarrow S_0$, $S_3 \leftarrow S_0$, and $S_5 \leftarrow S_0$ transitions, respectively, and we assign the features at 294.1, 282.2, and 248.4 nm in the $C_{17}H_{14}$ spectrum to the electronic origins of the $S_2 \leftarrow S_0$, $S_3 \leftarrow S_0$, and $S_5 \leftarrow S_0$ transitions, respectively. The relatively complex and broad spectral features in the spectra of the species containing the phenanthrene chromophore make assignments to vibronic transitions unreliable. However, we can tentatively assign the features at 287.6, 287.3, and 290.0 nm in the $C_{15}H_{10}$, $C_{16}H_{12}$, and $C_{17}H_{14}$ spectra to the first vibronic band within their respective $S_2 \leftarrow S_0$ transition. We can also tentatively assign the features at 243.8 and 240.6 nm in the $C_{16}H_{12}$ and $C_{17}H_{14}$ spectra to the first vibronic band within their respective $S_5 \leftarrow S_0$ transition.

In the same way that the closed-shell neutral species exhibit similar spectra, the open-shelled cations of the H_n-PAHs containing the phenanthrene chromophore also exhibit similar spectra. We can assign the features at 846.6, 995.9, and 872.7 nm in the respective $C_{15}H_{10}^{+}\cdot$, $C_{16}H_{12}^{+}\cdot$, and $C_{17}H_{14}^{+}\cdot$ spectra to their $D_2 \leftarrow D_0$ transition. As the $D_3 \leftarrow D_0$ transition is too weak to observe in the $C_{14}H_{10}^{+}\cdot$ spectrum, we do not observe any features in the phenanthrene chromophore–containing H_n-PAH cations that can be assigned to their respective $D_3 \leftarrow D_0$ transitions. Although the electronic transitions lying higher in energy exhibit weaker, broader, and more complex spectral features than the features associated with the $D_2 \leftarrow D_0$ transition, making definitive assignments difficult, we can tentatively assign the 500.3, 407.7, and 373.8 nm bands in the $C_{15}H_{10}^{+}\cdot$ spectrum to the origins of the $D_4 \leftarrow D_0$, $D_5 \leftarrow D_0$, and $D_6 \leftarrow D_0$ transitions, respectively; the 477.0, 431.5, and 403.3 nm bands in the $C_{16}H_{12}^{+}\cdot$ spectrum to the origins of the $D_4 \leftarrow D_0$, $D_5 \leftarrow D_0$, and $D_6 \leftarrow D_0$ transitions, respectively; and the 477.6, 434.9, and 403.5 nm bands in the $C_{17}H_{14}^{+}\cdot$ spectrum to the origins of the $D_4 \leftarrow D_0$, $D_5 \leftarrow D_0$, and $D_6 \leftarrow D_0$ transitions, respectively.

4.3. *Neutral and Ionized Pyrene* ($C_{16}H_{10}$), *7,8-dihydro-9H-cyclopenta[a]pyrene* ($C_{19}H_{14}$), *and 7,8,9,10-tetrahydrobenzo[a]pyrene* ($C_{20}H_{16}$)

The UV/visible spectroscopy of matrix-isolated pyrene, $C_{16}H_{10}$, and the pyrene cation, $C_{16}H_{10}^{+}\cdot$, has also been extensively studied (Salama & Allamandola 1992, 1993; Vala et al. 1994). The UV spectrum of $C_{16}H_{10}$ exhibits three dominant spectral features that have been assigned to the origins of the $S_2 \leftarrow S_0$, $S_3 \leftarrow S_0$, and $S_4 \leftarrow S_0$ transitions. The spectral positions of these features for the neutral species isolated in Ne matrices are observed at 323.3, 265.2, and 232.3 nm, respectively.

We observe four previously assigned electronic origins in the $C_{16}H_{10}^{+}\cdot$ spectrum. These are the $D_2 \leftarrow D_0$ origin at 781.6 nm,

TABLE 2

SPECTRAL DATA FOR THE PAH NEUTRAL MOLECULES AND CATIONS CONTAINING THE PHENANTHRENE CHROMOPHORE

Species	Assignment	Position (nm)	Shift (cm^{-1})	Maximum Absorbance
Phenanthrene ($C_{14}H_{10}$)	7 ← 0	214.5	0	0.084
	6 ← 0	229.0	...	0.261
		235.2	1365	0.661
	5 ← 0	243.0	0	1.000
	4 ← 0	262.4	0	0.087
		267.2	849	0.144
	3 ← 0	273.4	0	0.180
		281.2	388	0.147
	2 ← 0	284.3	0	0.748
4 *H*-Cyclopenta[*def*]phenanthrene ($C_{15}H_{10}$)		215.8	...	0.232
		220.8	...	0.224
		238.0	...	0.670
		241.4	...	0.760
	5 ← 0	245.2	0	0.852
	3 ← 0	279.6	0	0.298
		287.6	419	0.266
	2 ← 0	291.1	0	1.000
4,5-Dihydropyrene ($C_{16}H_{12}$)		209.7	...	0.348
		213.8	...	0.210
		218.0	...	0.202
		232.4	...	0.290
		243.8	1303	0.674
	5 ← 0	251.8	0	0.904
		274.7	...	0.220
	3 ← 0	278.9	0	0.306
		287.3	372	0.207
	2 ← 0	290.4	0	1.000
5,6-Dihydro-4 *H*-benz[*de*]anthracene ($C_{17}H_{14}$)		220.4	...	0.162
		233.9	...	0.340
		240.6	1305	0.727
	5 ← 0	248.4	0	1.000
		257.7	...	0.190
	3 ← 0	282.2	0	0.162
		290.9	374	0.162
	2 ← 0	294.1	0	0.428

Species	Assignment	Position (nm)	Shift (cm^{-1})	Maximum Absorbance
Phenanthrene cation ($C_{14}H_{10}^{+}$)	6 ← 0	396.0	0	0.068
	5 ← 0	425.8	0	0.077
	4 ← 0	470.7	0	0.068
		780.4	1682	0.085
		787.9	1560	0.128
		794.5	1455	0.128
		818.9	1080	0.051
		836.8	818	0.077
		856.6	542	0.274
		880.6	224	0.068
	2 ← 0	898.3	0	1.000
4 *H*-Cyclopenta[*def*]phenanthrene cation ($C_{15}H_{10}^{+}$)	6 ← 0	373.8	0	0.053
	5 ← 0	407.7	0	0.057
	4 ← 0	500.3	0	0.097
		751.3	1498	0.189
		761.4	1322	0.119
		806.8	583	0.256
	2 ← 0	846.6	0	1.000
4,5-Dihydropyrene cation ($C_{16}H_{12}^{+}$)	6 ← 0	403.3	0	0.084
	5 ← 0	431.5	0	0.084
	4 ← 0	477.0	0	0.048
		852.8	1685	0.120
		862.1	1559	0.108
		872.1	1426	0.108
		881.0	1310	0.084
		944.2	550	0.145
	2 ← 0	995.9	0	1.000
5,6-Dihydro-4*H*-benz[*de*]anthracene cation ($C_{17}H_{14}^{+}$)	6 ← 0	403.5	0	0.464
	5 ← 0	434.9	0	0.464
	4 ← 0	477.6	0	0.107
		754.1	1802	0.250
		759.5	1708	0.250
		767.0	1579	0.286
		778.1	1393	0.250
		837.6	480	0.143
		854.8	240	0.214
	2 ← 0	872.7	0	1.000

NOTE.—Only the most intense features observed are included here.

the $D_4 \leftarrow D_0$ origin at 483.3 nm, the $D_5 \leftarrow D_0$ origin at 438.7 nm, and the $D_6 \leftarrow D_0$ origin at 359.9 nm. Vala et al. have observed the spectral origin of the $D_3 \leftarrow D_0$ transition for $C_{16}H_{10}^+\cdot$ isolated in Ar matrices at 713.8 nm (Vala et al. 1994); this feature is presumably too weak to observe in the experiments reported here.

Like the H_n-PAHs containing the naphthalene and phenanthrene chromophores, the H_n-PAHs containing the pyrene chromophore also exhibit similar UV/visible spectra as compared to the pyrene molecule itself. Accordingly, we assign the 331.8, 271.1, and 238.0 nm bands in the $C_{19}H_{14}$ spectrum to the origins of the $S_2 \leftarrow S_0$, $S_3 \leftarrow S_0$, and $S_4 \leftarrow S_0$ transitions, respectively, and the 334.3, 271.6, and 238.6 nm bands in the $C_{20}H_{16}$ spectrum to the origins of the $S_2 \leftarrow S_0$, $S_3 \leftarrow S_0$, and $S_4 \leftarrow S_0$ transitions, respectively. Interestingly, as compared to the H_n-PAHs containing the naphthalene and phenanthrene chromophores, the majority of the vibronic bands observed in the $C_{19}H_{14}$ and $C_{20}H_{16}$ spectra are very similar in spacing to the pyrene molecule itself. This can be interpreted as being due to the "superaromatic" nature of the pyrene chromophore. Compared to the other series of compounds, the molecular orbitals that comprise the aromatic nature of the pyrene chromophore are not perturbed to a great extent by the aliphatic side chains.

In a similar manner, we assign the 758.7, 512.3, 447.5, and 369.6 nm bands in the $C_{19}H_{14}^+\cdot$ spectrum to the origins of the $D_2 \leftarrow D_0$, $D_4 \leftarrow D_0$, $D_5 \leftarrow D_0$, and $D_6 \leftarrow D_0$ transitions, respectively, and the 764.6, 513.6, 452.7, and 370.5 nm bands in the $C_{20}H_{16}^+\cdot$ spectrum to the origins of the $D_2 \leftarrow D_0$, $D_4 \leftarrow D_0$, $D_5 \leftarrow D_0$, and $D_6 \leftarrow D_0$ transitions, respectively. The spectral origin of the $D_3 \leftarrow D_0$ transition is presumably too weak to observe for these cations in the experiments reported here.

5. DISCUSSION—IMPLICATIONS FOR THE DIBs

The strong structural similarity found between the spectral signature of H_n-PAHs and that of their regular PAH counterparts in the near-UV to near-IR range leads to the same global conclusions regarding their potential astrophysical implications. As the known DIBs lie in the visible to near-IR region of the spectrum and the most intense spectral features of small neutral H_n-PAHs, such as the ones considered in this study, lie in the UV region, these species do not contribute to the DIBs. This is expected from the molecular size of these compounds (Salama et al. 1996). Their cationic forms (H_n-$PAH^+\cdot$), however, absorb in the optical range and may contribute to the DIBs. In Table 4, we compare the spectral positions of the H_n-PAH cations measured in Ne matrices with the positions of known DIBs from spectra of five reddened early-type stars selected from a recent DIB survey (Salama et al. 1999). The DIBs were chosen based on a 100 Å window around the laboratory peak wavelength positions. This criterion for the wavelength width was chosen to take into account the upper limit to the wavelength shift known to be induced by the solid matrix on isolated PAH ions (Salama et al. 1999; Ruiterkamp et al. 2002). This comparison indicates that $C_{19}H_{14}^+\cdot$ and $C_{20}H_{16}^+\cdot$ offer promising matches with known DIBs that would warrant gas-phase measurements in the laboratory for a definitive assessment. $C_{15}H_{10}^+\cdot$, $C_{16}H_{12}^+\cdot$, and $C_{17}H_{14}^+\cdot$ can be unambiguously excluded as potential DIB carriers, since their strongest absorption bands are not found in astronomical spectra. Finally, although the strongest absorption band of $C_{12}H_{10}^+\cdot$ comes close to a DIB (within the width of the chosen comparison window), recent gas-phase measurements that provide the unperturbed, intrinsic peak position for the band clearly show that $C_{12}H_{10}^+\cdot$ can also be unambiguously excluded as a DIB carrier (Biennier et al. 2004).

TABLE 4

Comparison of DIBs with the Absorptions of the PAH Cations Selected in This Study

λ PAH^+ (Ne matrix data)	DIBs[a]
3696 $C_{19}H_{14}^+$ (B)	...
3705 $C_{20}H_{16}^+$ (B)	...
4475 $C_{19}H_{14}^+$ (A)	DIB 4428.88
4527 $C_{20}H_{16}^+$ (A)	DIB 4501.8
6481 $C_{12}H_{10}^+$ (A)	DIB 6491.88
8466 $C_{15}H_{10}^+$ (A)	...
8727 $C_{17}H_{14}^+$ (A)	...
9442 $C_{16}H_{12}^+$ (A)	...

Notes.—Here 7,8-dihydro-9*H*-cyclopenta[*a*]pyrene is $C_{19}H_{14}^+$; 7,8,9,10-tetrahydrobenzo[*a*]pyrene is $C_{20}H_{16}^+$; Acenaphthene is $C_{12}H_{10}^+$; 5,6-dihydro-4*H*-benz[*d,e*]anthracene is $C_{17}H_{14}^+$; and 4,5-dihydropyrene is $C_{16}H_{12}^+$. A is the strongest absorption band in the NUV–NIR range, and B is the second strongest band. The positions of all spectral features are given in units of Å.

[a] The DIBs have been selected from 5 objects: HD 207198, BD +40 4220, HD 195592, HD 190603, and HD 187459 (see Salama et al. 1999).

6. CONCLUSIONS

According to the latest models (Le Page et al. 2003), the state of hydrogenation of PAHs strongly depends on the size of the molecule, with the degree of hydrogenation increasing with the size of the PAH. The laboratory matrix isolation studies reported here provide the first electronic and vibronic spectra of neutral and ionized H_n-PAHs for comparison with astronomical data. We show that the spectral characteristics of H_n-PAHs and their ions are very similar to the spectral characteristics of their regular PAH chromophores, yet are distinct enough to discern individual species in the ISM through their electronic excitation spectral signatures. This study also provides a guide to cavity ring-down spectroscopy (CRDS) follow-up measurements in the gas phase by preselecting the most promising molecular candidates. Thus, the same arguments adopted for comparison of regular PAH cations with the DIBs (Salama et al. 1999; Ruiterkamp et al. 2002) hold for their H_n-PAH cation counterparts. The spectral measurements taken in this study show that both fully aromatic PAH cations as well as H_n-PAH cations may contribute to the interstellar extinction and, in particular, to DIBs and UIR bands.

The authors would like to thank R. Walker for outstanding technical support. This work was supported by the Astronomy and Physics Research and Analysis (APRA) Program (RTOP 188-01-00-21) of NASA's Science Mission Directorate.

REFERENCES

Allamandola, L. J., Hudgins, D. M., & Sandford, S. A. 1999, ApJ, 511, L115
Arnoult, K. M., Wdowiak, T. J., & Beegle, L. W. 2000, ApJ, 535, 815
Bakes, E. L. O., Tielens, A. G. G. M., Bauschlicher, C. W., Jr., Hudgins, D. M., & Allamandola, L. J. 2001, ApJ, 560, 261
Banisaukas, J., et al. 2003, J. Phys. Chem. A, 107, 782
Bauschlicher, C. W., Jr. 1998a, Chem. Phys., 233, 29
———. 1998b, Chem. Phys., 234, 87
———. 1998c, ApJ, 509, L125

Bauschlicher, C. W., Jr. 2002, ApJ, 564, 782
Bauschlicher, C. W., Jr., & Bakes, E. L. O. 2001, Chem. Phys., 274, 11
Bauschlicher, C. W., Jr., Hudgins, D. M., & Allamandola, L. J. 1999, Theor. Chem. Accounts, 103, 154
Beegle, L. W., Wdowiak, T. J., & Arnoult, K. M. 1997a, ApJ, 486, L153
Beegle, L. W., Wdowiak, T. J., & Harrison, J. G. 2001, Spectrochim. Acta A, 57, 737
Beegle, L. W., Wdowiak, T. J., Robinson, M. S., Cronin, J. R., McGehee, M. D., Clemett, S. J., & Gillette, S. 1997b, ApJ, 487, 976
Bernstein, M. P., Sandford, S. A., & Allamandola, L. J. 1996, ApJ, 472, L127
Biennier, L., Salama, F., Allamandola, L. J., & Scherer, J. J. 2003, J. Chem. Phys., 118, 7863
Biennier, L., Salama, F., Gupta, M., & O'Keefe, A. 2004, Chem. Phys. Lett., 387, 287
Bréchignac, P., & Pino, T. 1999, A&A, 343, L49
Bréchignac, P., Pino, T., & Boudin, N. 2001, Spectrochim. Acta A, 57, 745
Chillier, X. D. F., Stone, B. M., Salama, F., & Allamandola, L. J. 1999, J. Chem. Phys., 111, 449
Duley, W. W., & Williams, D. A. 1981, MNRAS, 196, 269
Gillett, F. C., Forrest, W. J., & Merrill, K. M. 1973, ApJ, 183, 87
Halasinski, T. M., Hudgins, D. M., Salama, F., Allamandola, L. J., & Bally, T. 2000, J. Phys. Chem. A, 104, 7484
Herbst, E., & Le Page, V. 1999, A&A, 344, 310
Hudgins, D. M., Bauschlicher, C. W., Jr., & Allamandola, L. J. 2001, Spectrochim. Acta A, 57, 907
Hudgins, D. M., Bauschlicher, C. W., Jr., Allamandola, L. J., & Fetzer, J. C. 2000, J. Phys. Chem. A, 104, 3655
Jochims, H. W., Baumgartel, H., & Leach, S. 1999, ApJ, 512, 500
Jourdain de Muizon, M., Geballe, T. R., d'Hendecourt, L. B., & Baas, F. 1986, ApJ, 306, L105
Le Page, V., Keheyan, Y., Snow, T. P., & Bierbaum, V. M. 1999, Int. J. Mass Spectrom., 187, 949
Le Page, V., Snow, T. P., & Bierbaum, V. M. 2003, ApJ, 584, 316
Mattioda, A. L., Hudgins, D. M., Bauschlicher, C. W., Jr., Rosi, M., & Allamandola, L. J. 2003, J. Phys. Chem. A, 107, 1486
Pauzat, F., & Ellinger, Y. 2001, MNRAS, 324, 355
———. 2002, Chem. Phys., 280, 267
Petrie, S., Stranger, R., & Duley, W. W. 2003, ApJ, 594, 869
Pino, T., Boudin, N., Bréchignac, P. 1999, J. Chem. Phys., 111, 7337
Romanini, D., Biennier, L., Salama, F., Kachanov, A., Allamandola, L. J., & Stoeckel, F. 1999, Chem. Phys. Lett., 303, 165
Ruiterkamp, R., Halasinski, T., Salama, F., Foing, B. H., Allamandola, L. J., Schmidt, W., & Ehrenfreund, P. 2002, A&A, 390, 1153
Salama, F. 1996, in Low Temperature Molecular Spectroscopy, ed. R. Fausto (NATO ASI Series C, 483; Dordrecht: Kluwer), 169
Salama, F., & Allamandola, L. J. 1991, J. Chem. Phys., 94, 6964
———. 1992, Nature, 358, 42
———. 1993, J. Chem. Soc. Faraday Trans., 89, 2277
Salama, F., Bakes, E. L. O., Allamandola, L. J., & Tielens, A. G. G. M. 1996, ApJ, 458, 621
Salama, F., Galazutdinov, G. A., Krelowski, J., Allamandola, L. J., & Musaev, F. A. 1999, ApJ, 526, 265
Salama, F., Joblin, C., & Allamandola, L. J. 1994, J. Chem. Phys., 101, 10252
Schutte, W. A., Tielens, A. G. G. M., & Allamandola, L. J. 1993, ApJ, 415, 397
Sloan, G. C., Bregman, J. D., Geballe, T. R., Allamandola, L. J., & Woodward, C. E. 1997, ApJ, 474, 735
Snow, T. P. 2001, Spectrochim. Acta A, 57, 615
Snow, T. P., Le Page, V., Keheyan, Y., & Bierbaum, V. M. 1998, Nature, 391, 259
Vala, M., Szczepanski, J., Pauzat, F., Parisel, O., Talbi, D., & Ellinger, Y. 1994, J. Phys. Chem., 98, 9187
Wagner, D. R., Kim, H. S., & Saykally, R. J. 2000, ApJ, 545, 854
Weisman, J. L., Lee, T. J., & Head-Gordon, M. 2001, Spectrochim. Acta A, 57, 931
Weisman, J. L., Lee, T. J., Salama, F., & Head-Gordon, M. 2003, ApJ, 587, 256